Desalination and Water Treatment
www.deswater.com

doi: 10.5004/dwt.2017.20874

96 (2017) 193–200
November

Improvement of hydraulic loading rate by optimization of internal characteristics of dissolved air flotation

Min-Soo Meang, Young-Seok Hwang, Ki-Seok Lee, Seok Dockko*

Department of Civil and Environmental Engineering, Dankook University, 16890, Yongin-si, Gyeonggi-do, 448-701, Korea, Tel. +82-31-8005-3488; Fax: +82-31-8021-7213; emails: dockko@dankook.ac.kr (S. Dockko), minsoo13@dankook.ac.kr (M.-S. Meang), eangh02@naver.com (Y-S. Hwang), koreadream-ks@hanmail.net (K.-S. Lee)

Received 31 January 2017; Accepted 1 May 2017

ABSTRACT

The increasing concentration of phosphorous in the water system is presented as a cause of the algal bloom, which is spreading severely as the climate changes. It is therefore necessary to develop the technology to remove algae and phosphorus effectively. Dissolved air flotation (DAF) is effective in removing algae and phosphorous in water systems by using micro-bubbles. This study aims to increase the hydraulic loading rate by optimizing the internal hydraulic characteristics of the DAF process. The number of orifices in the nozzle has been diversified in order to optimize the volume and the size of micro-bubbles. Further, the slope baffle was optimized by enhancing the collision efficiency of micro-bubbles through the current control of the contact zone. An increase in the hydraulic loading rate as a function of the flow of the fluid was achieved by using a horizontal baffle and a perforated panel. According to the results of the tests, when the number of orifices in the nozzle is five, six, or seven, the diameter of the micro-bubbles decreases by approximately 37% and the bubble volume concentration increases by approximately 15%. In addition, the turbidity and T-P removal achieved were 96% and 98%, respectively. This represents increases of 28% and 23%, respectively, and was achieved by changing the height ratio of the slope baffle, including a horizontal baffle, and changing the perforation ratio of the perforation panel, as compared with the conventional DAF process.

Keywords: High-rate DAF; Orifice; Nozzle; Slope; Horizontal baffle; Perforated panel; Phosphorus

1. Introduction

Due to recent climate changes, the inordinate algal blooms are expected to decrease the treatment efficiency and increase the cost of water treatment plants (WTP). The taste and odor caused by the algae are causing apprehension in the use of tap water [1,2]. The sedimentary material such as phosphorous and nitrogen are deposited as internal pollutants at the bottoms of lakes. Due to climate change, dissolved oxygen at the bottom of a lake decreases and the release of phosphorus intensifies the algal bloom. Also, in raw water with low turbidity and non-precipitation matter, micro-flocs are slowly formed and deposited in the process of water treatment, making it difficult to deal with using conventional sedimentation methods. Dissolved air flotation (DAF) is an alternative technology for effective total phosphorus (T-P) and algae removal in an existing sedimentation process. The treatment time of DAF is less than one-eighth of that for conventional sedimentation processes. It was reported as an effective method for the removal of odor and taste, non-precipitation matters such as algae, and dissolved organic matter and nutritive salts such as T-P, when compared with coagulation/flocculation [3,4]. Moreover, DAF has the advantage of reducing the installation area of the WTP and simplifying the operation and maintenance of the treatment process through an automated process in

* Corresponding author.

Presented at the 9th International Conference on Challenges in Environmental Science & Engineering (CESE-2016), 6–10 November 2016, Kaohsiung, Taiwan.

comparison with conventional sedimentation processes [5,6]. The conventional DAF process is operated at a hydraulic loading rate of 5–15 m/h. However, high-rate DAF (HDAF) with a hydraulic loading rate of 30–50 m/h has appeared recently [7,8]. In the case of HDAF, an error in the design of the flotation zone will cause the bubble–flocs to flow out with the treated water because the hydraulic loading rate is faster than the rising velocity of bubbles. The flotation reactor consists of two parts: the contact zone and the flotation zone. In order to prevent an outflow situation, the ideal fluid pattern must be maintained within the flotation zone. In flotation zones, there are three characteristic flow patterns: the stratified flow on the surface, the plug flow in a vertical direction below the surface, and the plug flow in a horizontal direction in the bottom layer. It is known that when these types of flows are maintained, the DAF shows excellent performance [9–11]. In DAF, it is important to design the flotation tanks to have an optimized shape. This study aims to develop an HDAF process that is able to increase the hydraulic loading rate by means of internal configuration changes. The scope of the study is as follows: (1) the variation in internal configuration of the nozzle using HDAF, the analysis of bubble characteristics, and the optimization of treatment efficiency according to changes in location of the nozzle within the contact zone; (2) the analysis of treatment efficiency according to changes in the HDAF shape and height of slope baffle; (3) the analysis of the treatment efficiency by changing the length ratio of the horizontal baffle; and (4) evaluation of the treatment efficiency according to the distribution pattern of the perforated panel and the perforated rate.

2. Materials and methods

2.1. Synthetic water

The synthetic water that was used for the experiment was based on the water quality of lake water as shown in Table 1. $CH_3COONa_3H_2O$ (Daejung Chemicals, Korea) was used for pH adjustment, Bacto-yeast extract (Difco, USA) was used as a carbon source. Kaolin chemicals (Duksan Pure Chemical, Korea) were used for turbidity and suspended solids (SS). NH_4Cl (Daejung Chemicals, Korea) and K_2HPO_4 (Daejung Chemicals, Korea) were used for nitrogen and phosphorous, respectively.

Table 1
Quality of synthetic water

Lake water (real water)	Component	Synthetic water
COD_{cr}: 18 ± 0.5 mg/L	Bacto-yeast extract $CH_3COONa_3H_2O$	COD_{cr}: 20 ± 0.5 mg/L
SS: 73 ± 2 mg/L	Kaolinite	SS: 80 ± 2 mg/L
Turbidity: 35 ± 1 mg/L		Turbidity: 40 ± 1 mg/L
T-N: 8 ± 0.5 mg/L	NH_4Cl	T-N: 10 ± 0.5 mg/L
T-P: 2 ± 0.1 mg/L	K_2HPO_4	T-P: 4 ± 0.2 mg/L

2.2. Schematic of the HDAF process

The schematic of the HDAF process is shown in Fig. 1. Process chart of the HDAF consists of coagulation/flocculation, contact zone and flotation zone. The experiment was conducted by adjusting the hydraulic loading rate from 20 to 40 m/h using an 880 W pump (Wilo Co. Ltd., German). Synthetic water was injected to the DAF reactor after pretreatment with a coagulant. The HDAF process produced a shorter retention time of less than one-eighth the time of the conventional DAF process. The aspect ratio of the flotation zone was designed as a 1:1 square design, instead of the 1:12 existing aspect ratio, to deepen the depth of the reactor. The nozzle, which is the part where the initial influent of HDAF meets the bubbles, forces synthetic water in the direction opposite to the inflow to enhance the bubble–floc collision. With regard to the study elements, modification of the slope baffle increased the efficiency of the flotation, the short-circuiting of the upper flotation zone was controlled through varying the length of the horizontal baffle, and the perforated panel increased the hydraulic loading rate by changing the distribution pattern of the perforated panel and the perforated rate. Recycle ratio of HDAF was 15%.

2.3. Optimum dose of coagulant

In order to determine optimum dose of coagulant, the synthetic water was conducted through a jar tester (Phipps & Bird, USA). The jar test was conducted by measuring the turbidity and T-P concentration after stirring as rapid mixing at 130 rpm for 5 min, as slow mixing at 50 rpm for 15 min, and after 30 min of precipitation. Optimum dose of coagulant using DAF process is determined through conventional method. The coagulant used was polyaluminum chloride (PAC: $Al(OH)_3Cl$, 17%). Cation polymer (A-101P, Eyang Co. Ltd., Korea) was used as a coagulant additive to measure the optimum volume of coagulant. Also, in order to identify the treatment efficiency of the synthetic water, turbidity and T-P were analyzed, respectively. T-P concentration was analyzed using a spectrophotometer (Hach Co. DR5000TM, USA) and turbidity was measured using a turbidity meter (Hach Co. 2100N Turbidimeter, USA).

2.4. Measurement of micro-bubble size using a particle counter

To measure the size of the micro-bubble produced by the saturator and nozzle, an online particle counter (Chemtrac,

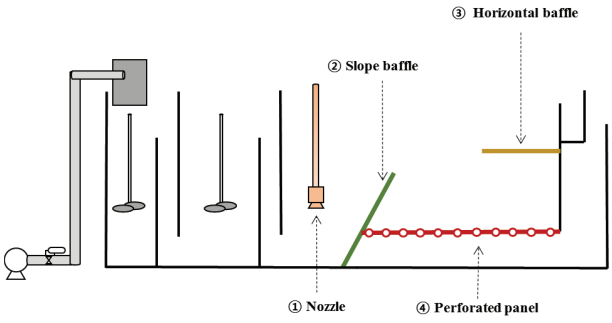

Fig. 1. Schematic of the HDAF process.

Model PC, USA) was used. The method of measuring bubble sizes using the counter equipment has been verified by other researchers [13]. Particle counter monitor (PCM) means measuring the distribution of sizes and numbers of bubbles by laser scattering in a particle counter. A schematic diagram of the measuring system is given in Fig. 2. For the same accuracy, PCM has a much shorter measuring time compared with conventional image analysis methods [12,13]. The measuring range covered eight channels and the bubble size was measured from 2 to 80 μm in increments of 10 μm. The injection flow was set at 100 mL/min.

2.5. Measurement of bubble volume concentration

The bubble volume concentration (BVC) was measured by the serial water substitution method using an acrylic reactor. After injecting pressurized water into the acrylic reactor using a volumetric pump, the volume of generated bubbles was measured using an air flow meter. The volume ratio of collected bubbles from the pressurized water was calculated as a dimensionless value.

2.6. Analysis of bubble characteristics in accordance with nozzle changes

As shown in Fig. 1, the nozzle of the HDAF process is the part where the pressurized water is sprayed through a saturator at atmospheric pressure. In general, the nozzle is fitted with a number of orifices and the bubble sizes and volume are changed according to their arrangement [14]. The number of nozzle orifices was changed from four to eight under the pressurized water condition and the same saturator. The sizes and the volumes of micro-bubbles were analyzed for the different nozzle configurations by PCM.

2.7. Effect of spray direction on micro-bubbles

In the normal DAF process, the flow of synthetic water and the spray direction of micro-bubbles are in the same direction. However, in this HDAF process, a reversed nozzle was applied to achieve micro-bubble flow in the opposite direction to the flow of the synthetic water. The collision capacity was enhanced by improving the combination of bubbles and floc through the forced increase in collisions. The ratio of flotation tank height vs. spray location (H_n/H) was changed from 0.125 to 0.25, 0.5, and 0.7 to further investigate the efficiency of bubble–floc combination. For evaluating the combination efficiency of the HDAF process, the location ratio of the optimum spray was decided by the removal of turbidity and T-P in the flotation zone.

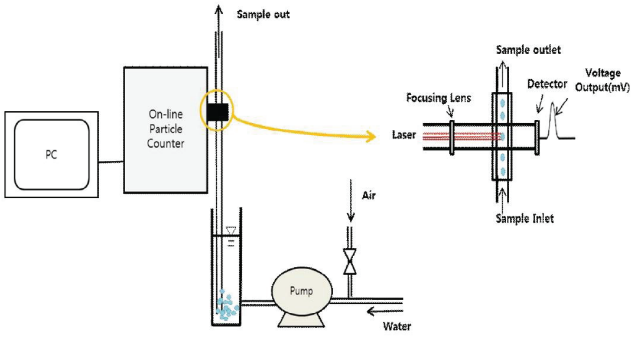

Fig. 2. Schematic diagram of PCM [12].

2.8. Effect of the slope baffle

The slope baffle increases the flotation capacity of particles by raising the surface area of synthetic water contacting with micro-bubbles in the flotation zone. To prevent short circuiting flow at the flotation zone, the height ratio of the slope baffle and the shape should be controlled. Various studies have been conducted by several researchers on the height ratio of the slope baffle and the shape [9,11,15]. As shown in Table 2, three height ratios of the slope baffle and two shape types were used.

2.9. Effect of the horizontal baffle

As the hydraulic loading rate increases in the conventional flotation zone, cases of short circuiting flow in the zone after the slope baffle have been reported [10]. The shear force generated in the flotation zone causes the lowest water quality in bubble–floc treatment. Therefore, to achieve effective flotation, it is necessary to control the upper part flow using a horizontal baffle. Fig. 3 shows the effect of each baffle by changing the ratio of the horizontal baffle (W_b/W) from 0.165 to 0.33 and 0.495, in terms of surface area of the flotation zone.

2.10. Effect of the perforated panel

A previous study reported that the flow at the bottom part of the flotation zone (B zone) shows a fast velocity distribution as it is close to the outlet, and it showed irregular fluid flow by the short-circuiting flow [15]. Parts of the sludge are spilled

Table 2
Height ratio of slope baffle as a function of baffle

Type	Height ratio (H_s/H)		
	0.55	0.65	0.75
Linear slope baffle	L55	L65	L75
Bend slope baffle	B55	B65	B75

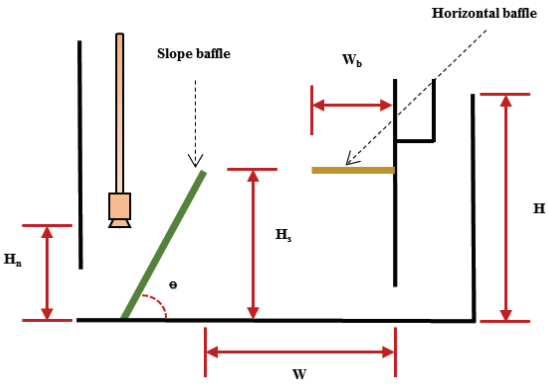

Fig. 3. (H_n/H) of flotation zone, (H_s/H) of slope baffle, and (W_b/W) of horizontal baffle.

into the lower part of the flotation zone and increase the turbidity of the treated water. Therefore, a porous perforated panel was used to decrease the occurrence of short-circuiting flow, as shown in Fig. 4. Table 3 presents the results of this experiment, which was conducted by changing the perforation ratio and the perforation arrangement of each panel.

2.11. Computational fluid dynamics analysis of the HDAF process

To analyze the HDAF process using computational fluid dynamics (CFD), the ANSYS Fluent V.16.5 program was used. The HDAF process was analyzed as two-phase flow of water and bubbles and the characteristics of the fluid flow according to internal configuration changes were identified. To identify the characteristics of fluid flow, a k–ε turbulent model was applied. With the application of the k–ε turbulent model, the result of the computational analysis is more representative than the result of a numerical analysis assuming laminar flow [16,17]. Therefore, this analysis was conducted by applying the k–ε turbulent model. The influent of synthetic water and pressurized water were adjusted in terms of inlet velocity. The treated water was adjusted in terms of outlet pressure. The boundary conditions for this analysis were as indicated in Table 4.

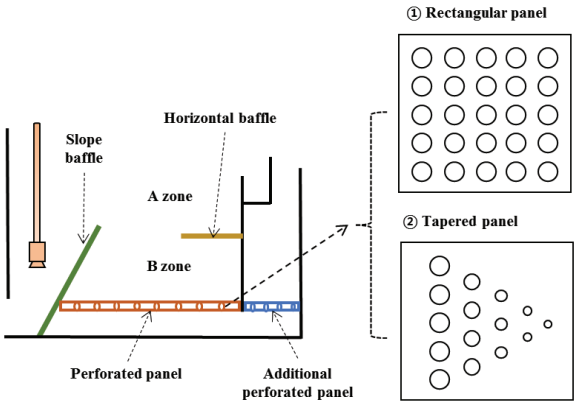

Fig. 4. Perforated panel in flotation zone.

Table 3
Perforation ratio of perforated panel as a function of panel

Type	Perforation ratio		
	0.25	0.50	0.75
Rectangular panel	H25	H50	H75
Tapered panel	T25	T50	T75

Table 4
Configuration of HDAF

Location	Boundary condition
Influent	Velocity inlet
Inflow of pressurized water	Velocity inlet
Effluent of treated water	Pressure outlet
Wall	No slip

3. Results and discussion

3.1. Bubble size and BVC depending on number of nozzle orifices

Fig. 5 shows the distribution of bubble size against the number of bubbles as a function of the number of orifices in the nozzle. Four, six, and eight orifices were used. Most of the generated bubbles had a size of 10–30 μm. The results also show that the average bubble size decreases as the number of orifices increases. In addition, the generation of bubbles over 50 μm also decreases.

Previous researcher shows that optimum the number of orifice is dependent on specific flow rate generated in the DAF system [18].

Table 5 indicates that the optimum BVC is 69 mL/L when six orifices are used. The flotation time was 115 s, which was an increase of 40% over conventional DAF [14]. This means that the decrease in bubble size also decreases the flotation velocity and increases the retention time of the bubble flotation layer, which is significant for treated water.

3.2. CFD analysis of the HDAF process

Fig. 6(a) shows the velocity distribution over the optimum slope baffle at a hydraulic loading rate of 30 m/h.

The bubble–floc which passed over the slope baffle is spilled through the outlet immediately due to the high velocity of the bubbles caused by the high hydraulic loading rate.

The flow structure was found to be matter of a limiting distance between the slope baffle top and the drainage pipe, and between the top of the slope baffle and the water surface [19].

Fig. 6(b) shows that the treatment efficiency of the DAF process with a horizontal baffle installed has been improved without immediate spillage by inducing the retention of flow at the upper part. However, even with the horizontal baffle, short-circuiting flow still occurred, and this decreased the treatment efficiency at the bottom part of the flotation zone. Therefore, as shown in Fig. 7, the treatment efficiency of the DAF process was improved by increasing the retention time due to the effect of suppressing the water flow with the perforated panel.

3.3. Effect of spray location on micro-bubbles

Fig. 8 shows the effect of hydraulic loading rate in accordance with changes in nozzle location and direction.

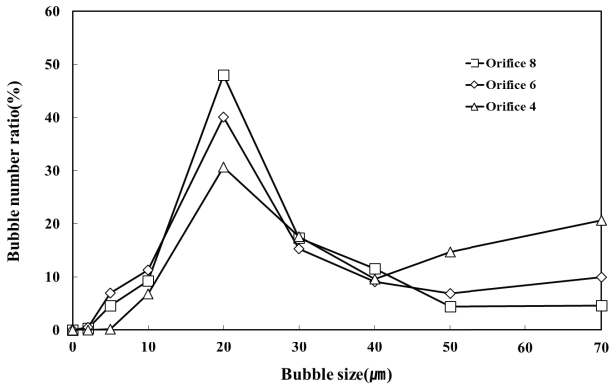

Fig. 5. Bubble size vs. bubble number ratio as a function of the number of orifices.

The ratio of nozzle location and the depth of the reactor was changed from 0.125 to 0.25, 0.5, and 0.7. Turbidity and T-P removal are indicated for hydraulic loading rates of 20, 30, and 40 m/h, respectively. The variation in the effects caused by changing the nozzle location was within 5% at 20 m/h. The optimum H_n/H was 0.25, and the removal of turbidity and T-P was 89.5% and 94.1%, respectively. However, as the hydraulic loading rate increased, the difference of removal rate in respect of H_n/H increased. At a hydraulic loading rate of 30 m/h, total efficiency was decreased and the removal of HDAF was the most when H_n/H was 0.5. When the hydraulic loading rate was 40 m/h, the optimum H_n/H was 0.7. As the hydraulic loading rate increased, the activation area of enhanced collision also increased.

3.4. Effect of the slope baffle

The optimum shape of the slope baffle was the linear for a hydraulic loading rate of 30 m/h, as shown in Fig. 9. This means that the shape of the slope baffle is effective for flotation separation if the water current flows are stable in the flotation zone after the contact zone [10,15]. Moreover,

Table 5
Bubble characteristics of HDAF

	HDAF nozzle			Conventional nozzle
	Orifices: 4	Orifices: 6	Orifices: 8	
Average bubble size (μm)	45.4	34.2	31.5	41.2
Bubble volume concentration (mL/L)	54	69	63	55
Flotation time of bubble in the reactor (s)	84	115	124	75

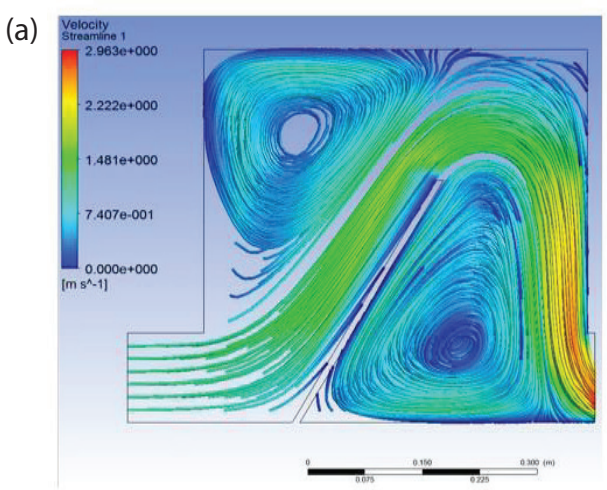

Fig. 6. Results of CFD analyses for (a) slope baffle and (b) slope baffle and horizontal baffle.

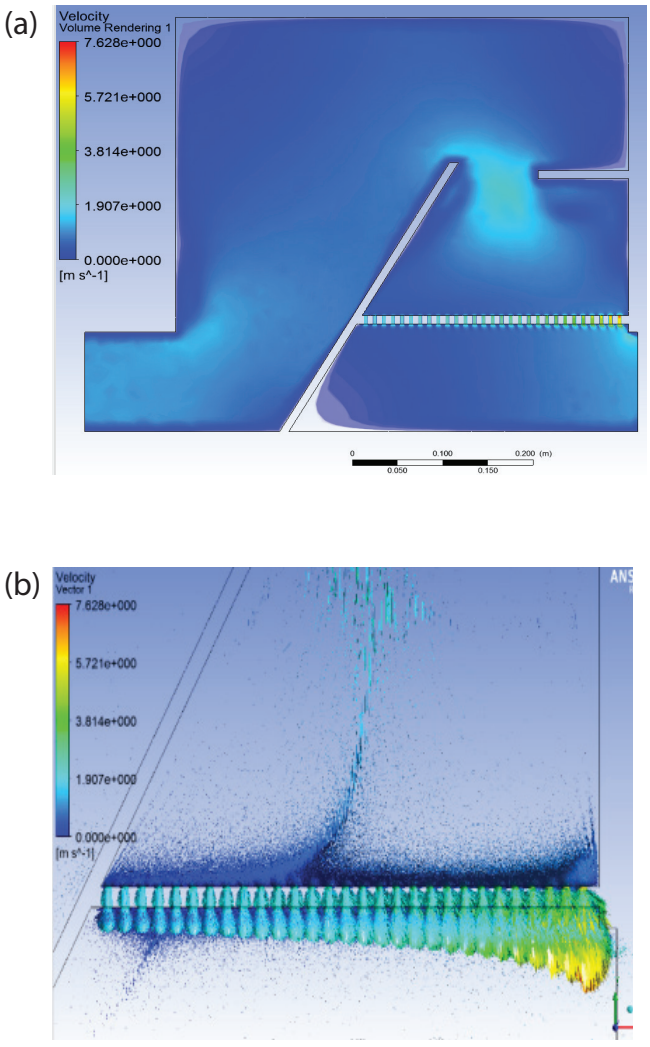

Fig. 7. Results of CFD for perforated (a) rectangular panel and (b) tapered panel.

bubble–flocs should be injected into the bottom part of the bubble-forming layer where flotation and separation occur simultaneously. Therefore, the optimum height ratio (H_s/H) of the slope baffle in the HDAF reactor is 0.65 and the removal of turbidity and T-P showed is 69.1% and 74.8%, respectively.

3.5. Effect of the horizontal baffle

Fig. 10 shows the treatment efficiency according to the length ratio of the horizontal baffle at the flotation zone, when height ratio H_s/H of the linear slope baffle was 0.165. According to previous research [20], velocity distribution with break-through flow was occurred as the velocity increased. In order to decline break-through flow, horizontal baffle was required to install in flotation zone. Therefore, the horizontal baffle increased the treatment efficiency of DAF by retaining bubble–flocs at the upper part after the slope baffle. With a length ratio of the horizontal baffle of 0.33, optimum treatment efficiency was achieved. When the length of the horizontal baffle shortened, the velocity at the upper part, which maintains the bubble layer, decreased. With a longer horizontal baffle, the velocity was increased because of the short distance between the slope baffle and the horizontal baffle. Immediate spillage of bubble–flocs then occurred and the treatment efficiency was decreased. Using the horizontal baffle with the optimum length ratio, T-P removal was 80.1%, which is 5.3% more than with only the slope baffle.

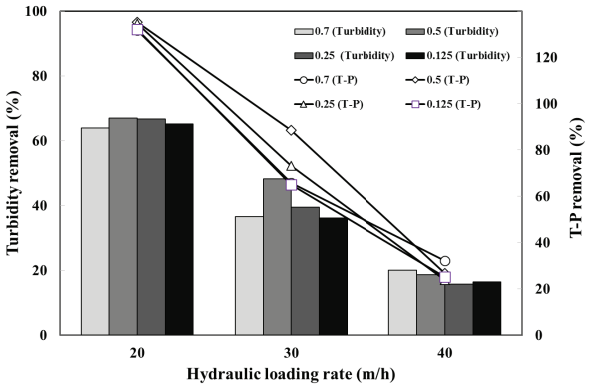

Fig. 8. Turbidity and T-P removal as a function of hydraulic loading rate and nozzle location.

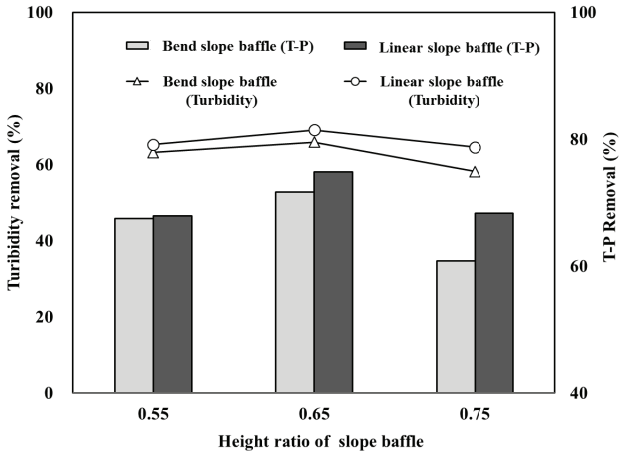

Fig. 9. Turbidity and T-P removal as a function of the height ratio of the slope baffle (hydraulic loading rate: 30 m/h).

3.6. Effect of the perforated panel

Therefore, Fig. 11 shows the results of the perforated panel on treatment efficiency based on the perforated panel

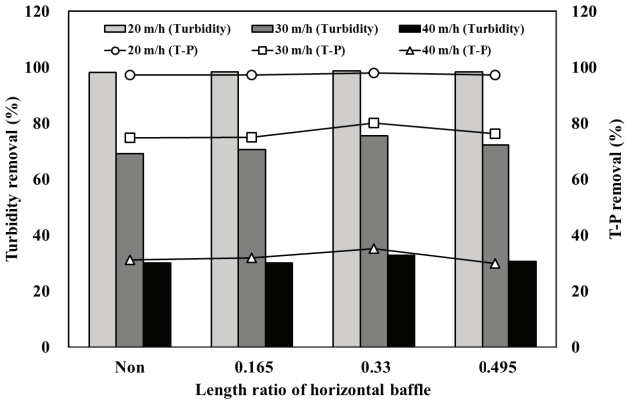

Fig. 10. Turbidity and T-P removal as a function of the length ratio of the horizontal baffle.

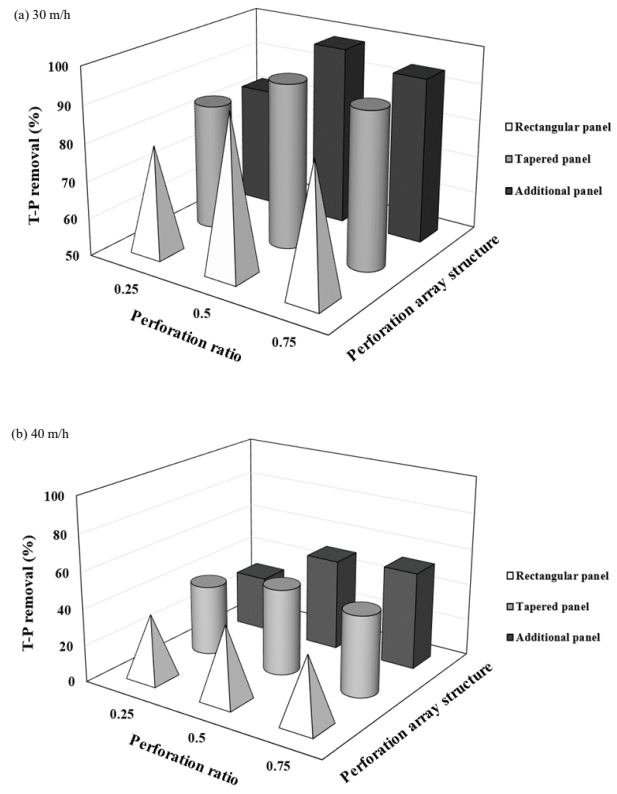

Fig. 11. T-P removal as a function of the perforation ratio and perforation array structure of perforated panels for (a) 30 m/h and (b) 40 m/h.

ratio and perforation arrangement, and for hydraulic loading rates of 30 and 40 m/h, respectively. It is reported that perforated panel was used as the effect of evenly distribution the flow [21]. When the hydraulic loading rate was 30 m/h, Fig. 11(a), the optimum perforation ratio was 0.5, regardless of the perforated panel arrangement. The treatment efficiency of DAF was increased with the tapered type, and the addition of an additional tapered type showed the highest treatment efficiency. The T-P removal achieved was 98.0%. When the hydraulic loading rate was 40 m/h, Fig. 11(b), the flotation capacity of the bubble layer decreased inside the flotation zone as the inflow of water increased in the reactor. Therefore, the optimum perforation ratio increased and did not affect the bubble layer. The optimum treatment efficiency was achieved when the perforation rate was 0.75 and the perforation arrangement was also tapered. Turbidity and T-P removal achieved were 49.1% and 53.2%, respectively.

3.7. Effect of total shape change

Fig. 12 shows the results for T-P and turbidity removal for a hydraulic loading rate of 30 m/h, as a function of changing the slope baffle, the horizontal baffle, and the perforated panel. In zone A, the treatment efficiency gradually increased for height ratios of 0.75, 0.55, and 0.65 for the slope baffles of bent type. The optimum slope baffle height ratio was 0.65 with a linear slope baffle. In zone B, the treatment efficiency showed higher removal of T-P than turbidity for both zones A and B for horizontal baffle length ratios of 0.165, 0.49, and 0.33. For zones C and D, the highest treatment efficiency was achieved when the perforation ratio of the perforated panel was 0.5. The tapered type perforation arrangement showed better results than the homogeneous type. The addition of a second perforated panel also showed higher treatment efficiency than with a single perforated panel. As a result, the optimum HDAF shape was shown to be when the slope baffle type, baffle length ratio, horizontal baffle length ratio, perforated panel, and perforation ratio were linear slope baffle, 0.65, 0.33, additional tapered panel, and 0.5, respectively. The treatment efficiency of this HDAF process showed turbidity and T-P removal as 96.2% and 98.0%, respectively.

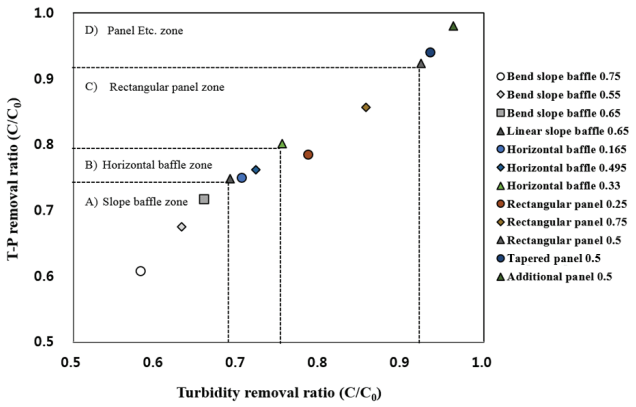

Fig. 12. Turbidity and T-P removal as a function of types of slope baffle, horizontal baffle, and perforated panel (30 m/h).

4. Conclusion

HDAF is an effective process to remove turbidity and T-P more effectively than conventional DAF for high hydraulic loading rates. However, various internal characteristics are required to achieve HDAF. The nozzle, as the basis of the DAF process, shows that the average bubble size decreases when the number of orifices increases. Most of the generated bubbles had a size of 10–30 μm. The optimum BVC was 69 mL/L when the number of orifices was six. A horizontal baffle increases the treatment efficiency of DAF by retaining bubble–flocs at the upper part after the slope baffle. The tapered type perforation arrangement showed better results than the homogeneous type. An additional perforated panel showed higher treatment efficiency than with a single perforated panel.

Acknowledgment

This research was supported by Korea Ministry of Environment (MOE) as "Global Top Project (2016002110007)".

References

[1] J.W. Yang, A study on the behavior of water quality using density current generator (DCG) in a lake – focused on DO, temperature, salinity, J. Korean Soc. Urban Environ., 11 (2011) 49–55.
[2] B.M. Ki, A study on the effects of the nutrient release from sediments in the reservoir, J. Korean Soc. Environ. Eng., 33 (2011) 553–563.
[3] Y. Liu, Q. Cheng, B. Zhang, F. Tian, Three-phase hydrocyclone separator: a review, Chem. Eng. Res. Des., 100 (2015) 554–560.
[4] J.R. Radman, R. Langlois, T. Leadbeater, J. Finch, N. Rowson, K. Waters, Particle flow visualization in quartz slurry inside a hydrocyclone using the positron emission particle tracking technique, Miner. Eng., 62 (2014) 142–145.
[5] R.K.L. Yap, M. Whittaker, M. Diao, R.M. Stuetz, B. Jefferson, V. Bulmus, W.L. Peirson, A.V. Nguyen, R.K. Henderson, Hydrophobically-associating cationic polymers as micro-bubble surface modifiers in dissolved air flotation for cyanobacteria cell separation, Water Res., 61 (2014) 253–262.
[6] J. Haarhoff, K. Edzwald, Adapting dissolved air flotation for the clarification of seawater, Desalination, 311 (2013) 90–94.
[7] J. Gasperi, B. Laborie, V. Rocher, Treatment of combined sewer overflows by ballasted flocculation: removal study of a large broad spectrum of pollutants, Chem. Eng. J., 211–212 (2012) 293–301.
[8] P. Jarvis, P. Buckingham, B. Holden, B. Jefferson, Low energy ballasted flotation, Water Res., 43 (2009) 3427–3434.
[9] C. Bhondayi, M.H. Moys, D. Fanucchi, G. Danha, Numerical and experimental study of the effect of a froth baffle on flotation cell performance, Miner. Eng., 77 (2015) 107–116.
[10] M. Bondelind, S. Sasic, M. Kostoglou, L. Bergdahl, T.J. Pettersson, Single- and two-phase numerical models of dissolved air flotation: comparison of 2D and 3D simulations, Colloids Surf., A, 365 (2010) 137–144.
[11] G.N. Ryu, S.M. Park, H.I. Lee, M.K. Chung, Numerical study of effect of DAF-tank shape on flow pattern in separation zone of dissolved air flotation, Trans. Korean Soc. Mech. Eng. B, 35 (2011) 855–860.
[12] M.Y. Han, Y.H. Park, J. Lee, J.S. Shim, Effect of pressure on bubble size in dissolved air flotation, Water Sci. Technol., 2 (2002) 41–46.
[13] M.R. Park, M.Y. Han, Evaluation of design parameters on microbubble generating device for control of bubble size, J. Korean Soc. Environ. Eng., 1 (2012) 242–243.
[14] S.C. Park, H.Y. Oh, M.K. Chung, S.L. Song, Y.H. Ahn, An effect of the micro bubble formation depending on the saturator and

the nozzle in the dissolved air flotation system, J. Korean Soc. Environ. Eng., 35 (2013) 929–936.
[15] B. Lakghomi, Y. Lawryshyn, R. Hofmann, A model of particle removal in a dissolved air flotation tank: importance of stratified flow and bubble size, Water Res., 68 (2015) 262–272.
[16] A. Wang, X. Yan, L. Wang, Y. Cao, J. Liu, Effect of cone angles on single-phase flow of a laboratory cyclonic-static micro-bubble flotation column: PIV measurement and CFD simulations, Sep. Purif. Technol., 149 (2015) 308–314.
[17] A.M. Goula, M. Kostoglou, T.D. Karapantsios, A.I. Zouboulis, A CFD methodology for the design of sedimentation tanks in potable water treatment. Case study: the influence of a feed flow control baffle, Chem. Eng. J., 140 (2008) 110–121.
[18] S.I. Oh, An Experimental Study on the Generation of Micro-Bubble Using Orifice Nozzle and the Flow Pattern of Bubbles in a DAF, M.S. Dissertation, Kumoh National Institute of Technology, Gumi, Korea, 2015.
[19] M. Lundh, L. Jonsson, J. Dahlquist, The influence of contact zone configuration on the flow structure in an dissolved air flotation pilot plant, Water Res., 36 (2002) 1585–1598.
[20] M. Lundh, L. Jonsson, J. Dahlquist, Experiment studies of the fluid dynamics in the separation zone in dissolved air flotation, Water Res., 34 (2000) 21–30.
[21] G.N. Ryu, S.M. Park, H.I. Lee, M.K. Chung, Numerical Study of the Effect DAF-Tank Shape on the Flow Pattern in the Separation, Trans. Korean Soc. Mech. Eng. B, 35 (2010) 855–860.